Interfacial Phenomena and Heat Transfer, 1 (3): 231–243 (2013)

DIFFUSION AND EVAPORATION CONTROL THE SPREADING OF VOLATILE DROPLETS ONTO SOLUBLE FILMS

Julien Dupas,[1] Emilie Verneuil,[1,*] Laurence Talini,[1] François Lequeux,[1] Marco Ramaioli,[2] & Laurent Forny[2]

[1]*PPMD-SIMM, UMR 7615, CNRS, UPMC, ESPCI ParisTech, 10 rue Vauquelin, 75231 Paris, France*

[2]*Nestle Research Center, Route du Jorat 57, 1000 Lausanne 26, Switzerland*

[*]Address all correspondence to Emilie Verneuil, E-mail: emilie.verneuil (at) espci.fr

The spreading dynamics of a water droplet on a soluble polymer substrate is controlled by the rate of water transfers into the substrate. We provide a comprehensive description of the parameters controlling the wetting dynamics based on the analysis of the transfers between the spreading liquid and the solid substrate. Our model is supported by experimental results obtained on supported films of polymer with thickness e varied over two decades, on which droplets of water spread with a velocity U spanning two decades. Three different transfers are governing the hydration dynamics: (i) Water evaporates from the droplet, condenses on the substrate, and further diffuses through the polymer. (ii) Liquid water at the contact line diffuses in the polymer ahead of the contact line. (iii) Water in the droplet is convected at the droplet velocity U. The evaporative process is the most efficient at hydrating the substrate and controls the hydration of the polymer at distances ranging between a macroscopic cutoff length L and a microscopic length κ. L is set by the diffusion of vapor in air. κ results from a balance between the diffusion of water from the droplet at the contact line and the diffusion of water in the atmosphere. By analyzing the hydration profile at all distances to the contact line between L and κ, we define three different spreading regimes: a thick film regime where the film behaves as a semi-infinite medium, a thin film regime where hydration is homogeneous along the film thickness, and an intermediate regime where both situations coexist along the film away from the contact line.

KEY WORDS: *dynamic, wetting, droplet, evaporation, solvent, polymer*

1. INTRODUCTION

Understanding the wetting properties is of fundamental importance in a number of practical applications, such as formulation of dispersions and suspensions (e.g., paints), design and process of coatings (e.g., for textile or glass), or lubrication. Beyond the classical case of a rigid solid wet by a simple viscous liquid (de Gennes, 1985; Leger and Joanny, 1992), a wide variety of static and dynamic behaviors arises when complex liquids and solids are considered. In particular, some efforts have been devoted to the cases of polymeric solids such as soft elastomer substrates (Long et al., 1996; Carre and Shanahan, 1995; Chen et al., 2013) or soluble polymers (Muralidhar et al., 2011; Tay et al., 2011a,b). In this paper, we focus on the spreading dynamics of water droplets onto hygroscopic polymer films. This problem is relevant to many different common situations such as soluble food products immersed in water or water droplets sprayed onto soluble solids. Recent works on the wetting of polymer substrates have evidenced the role played by different dynamical effects at a molecular scale with various origins: glass transition (Zuo et al., 2013), onset of a gel phase and viscoelastic effects (Kajiya et al., 2011, 2013), or flipping of the hydrophobic groups at the polymer/air interface toward the bulk upon wetting by a liquid (Monteux et al., 2009). Different models accounting for

2152–5080/13/$35.00

these dynamic effects at the contact line were developed to describe the wetting kinetics of a liquid droplet spreading onto a polymer film. Here, we develop another approach based on the analysis of the mass transfers at the interfaces to account for the spreading dynamics of a water droplet onto a soluble polymer film.

As a starting point, we recall the classical hydrodynamic model for moving liquid/solid contact lines on rigid, nonsoluble solids (de Gennes, 1985; Leger and Joanny, 1992), in situations of partial wetting and negligible gravity. The dynamics of wetting is determined by a balance between capillary and viscous forces. For small contact angles, using the lubrication approximation, the flow inside the droplet can be approximated by a Poiseuille flow and the resulting viscous dissipation is given by $3\eta U^2 \ln(R/a)/\theta$, where U is the spreading velocity, η is the viscosity of the liquid, θ is the dynamic contact angle, and R/a is the ratio of the droplet radius R and a microscopic length a. Note that the cutoff length a arises from the divergence of the shear stress in the liquid wedge in the vicinity of the contact line. Upon spreading, the dynamic contact angle is larger than its value at equilibrium θ_e, which is given by the Young's relation $\cos\theta_e = (\gamma_s - \gamma_{sl})/(\gamma)$, where γ_s, γ_{sl}, and γ are, respectively, the surface tensions of the air/solid, solid/liquid, and liquid/air interfaces. The resulting driving force is given by a balance of the horizontal capillary forces, yielding $F = \gamma\,(\cos\theta_e - \cos\theta)$. By balancing the viscous and capillary energies, the spreading velocity and the contact angle are related through: $(\cos\theta_e - \cos\theta)\,\theta = 3(\eta U)/(\gamma)\ln(R/a)$. This latter equation can be approximated for small angles θ by

$$\theta^3 \sim \theta_e^3 + 6\frac{\eta}{\gamma} U \ln\left(\frac{R}{a}\right). \tag{1}$$

Our recent works (Tay et al., 2010, 2011; Dupas et al., 2013) on soluble substrates have demonstrated that the spreading of a solvent on a soluble solid amounts to an increase of the substrate energy ahead of the contact line due to the transfers of the solvent in the material surrounding the droplet. In Eq. (1), an increase of the substrate energy corresponds to a decrease in the equilibrium contact angle θ_e and to a reduced dynamic contact angle θ for a given spreading velocity U.

In a recently published paper (Dupas et al., 2013), the case of thin polymer films wet by a water droplet was analyzed in detail. The contact angle was proved to be set by the volume fraction of water in the substrate in the immediate vicinity of the contact line. The study was restricted to polymer films with thicknesses e such that the water content of the film in the vertical direction was homogeneous, so that the problem was reduced to a one-dimensional (1D)-problem. We showed that water transfers into the polymer film through two mechanisms: (i) Water evaporates from the droplet, diffuses through the air, and condenses onto the film/air interface. (ii) Water diffuses from the droplet at the liquid/solid interface into the polymer. Transfer (i) was proven to be the most efficient, while transfer (ii) affects the water content in the very vicinity of the contact line over a typical distance of the order of the thickness of the film.

Herein we generalize our approach to polymer films of different thicknesses. We present systematical measurements of the dynamic contact angle with the parameters relevant to the transfers. We show that the hydration rate remains the key factor that controls the spreading dynamics. We identify different spreading regimes based on the relative magnitude of the transfers of water into the substrate at stake during the motion of a droplet. We map out these regimes both theoretically and experimentally, depending on the initial hydration degree of the polymer, the polymer film thickness, and the spreading velocity of the droplet. The results are summarized in a refined diagram based on the theoretical work of Tay et al. (2010) that describes the different wetting regimes. The paper is organized as follows. In a first section we summarize the main theoretical findings by Tay et al. (2010). The second section is devoted to the experimental procedures, and is followed by a presentation of our main results and their discussion as compared to the theoretical predictions. We finally provide a refined version of the wetting diagram and show that it is well supported by the results of the wetting experiments.

2. THEORETICAL BACKGROUND

In a theoretical analysis published earlier (Tay et al., 2010), three spreading regimes were identified by taking into account the water transferring by evaporation from the droplet and its condensation onto the polymer film, and the effect of the contact line movement at velocity U. The model does not include the third transfer which is the diffusion of liquid water from the droplet into the polymer at the contact line. In Fig. 1, a schematic representation of the

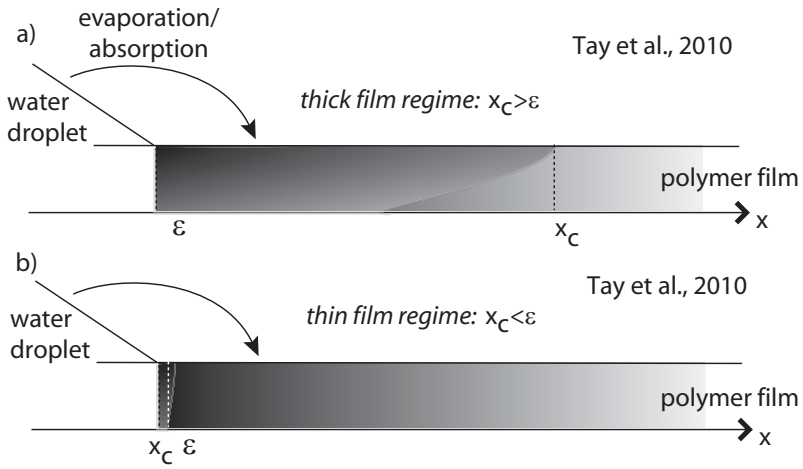

FIG. 1: Schematic representation of the water content in the layer ahead of the contact line, in the frame of reference of the droplet in the case where evaporation/absorption only is hydrating the film as described by Tay et al. (2010): (**a**) thick-film regime. (**b**) thin-film regime. The diffusion of vapor from the atmosphere penetrates and homogenizes over a distance to the contact line in the vertical direction that is larger than the film thickness for distances larger than x_c. For smaller distances, the film exhibits a vertical gradient of water content.

hydration by the evaporation/condensation process depicts the situation considered by Tay et al. (2010). Here we briefly recall the main results.

The water uptake depends on the spreading velocity U: the larger the velocity, the smaller the water uptake by the substrate since the less time it is in contact with humid air. Water uptake also depends on the thickness e of the substrate: the thinner the substrate, the larger the volume fraction in water for the same water uptake by the substrate. Tay et al. (2010) have therefore summarized the different spreading regimes in an e-U diagram. They first determined the high-velocity regime, where the solvent uptake in the substrate is negligible, the "dry regime," and regimes where the solvent uptake is substantial. The critical velocity separating those regimes is thickness independent and is given by $U_c = (D_v^2 c_{\mathrm{sat}}^2)/(D\rho^2\epsilon)$, where D_v is the diffusion coefficient of vapor in the air, c_{sat} is the saturation concentration of the solvent vapor in air, ρ is the density of the liquid solvent, D is the mutual diffusion coefficient of solvent in the polymer, and ϵ is a microscopic cutoff distance.

Within the "wet" cases, the film thickness e determines two different regimes where the hydration is substantial: (i) A thick-film regime, where the bottom of the layer is not "seen" by the water diffusing through the polymer from its interface with the atmosphere. The hydration exhibits a diffusive profile along the vertical direction, with a contact angle of the droplet on the substrate that is independent of the film thickness e [Fig. 1(a)]. (ii) A thin film regime where hydration is uniform across the film thickness, with no gradients of water volume fraction in the vertical direction [Fig. 1(b)]. At a given location along the x axis, the total amount of water that has condensed on the film diffuses through the polymer to a given depth before the droplet arrives and spreads onto that location. If the point of interest is located at a large enough distance to the contact line, the penetration depth of the condensed water exceeds the film thickness and then the hydration is uniform across the film thickness. Note that hydration always decreases along the x axis, away from the contact line. Hence, a critical distance arises x_c that separates the areas of the film where condensed water is allowed to diffuse across the whole thickness of the film e, while closer to the line, the water penetration is limited to the upper part of the film. Hence defined, $x_c = e^2U/D$. By comparing x_c to the other relevant lengths of the problem, Tay et al. (2010) were able to discriminate between the hydration regimes.

In particular, x_c was compared to a cutoff length ϵ of molecular size to discriminate the thick regime from the thin regime. The choice of this cutoff length was driven by the assumption that the contact angle is set by the degree of hydration of the polymer at some nanometric distance ϵ to the line, which should set the distance at which hydration ahead of the line tunes the wetting dynamics. The transition from the thin regime to the thick regime were thought to

happen for film thicknesses e such that $x_c = \epsilon$, that is, $e > \sqrt{(\epsilon D)/U}$. In both thin and thick regimes, the contact angle is set by the degree of hydration in the vicinity of the contact line. As a result, within the thick-film regime, θ is expected to be independent of the film thickness e, whereas in the thin film regime, θ is a function of the product of the thickness by the velocity eU, since the water volume fraction at the contact line scales with the product eU. Experimentally, it was shown (Tay et al., 2011; Dupas et al., 2013) that in the thin-film regime the dynamic contact angle varies as $1/(eU)$, in agreement with the theoretical predictions. However, a detailed analysis of the thin-film regime (Dupas et al., 2013) showed that the nanometric cutoff length ϵ suggested by Tay et al. (2010) was not relevant and that, close to the contact line, water transfer resulting from diffusion has to be considered. In the following section, we present our experimental results obtained on a large range of thicknesses that further demonstrate the need to include both transfers in the theoretical description of the phenomena, as detailed in the Discussion section.

3. EXPERIMENTAL SET-UP

3.1 Materials

The polymer used is a maltodextrin, a polysaccharide consisting of D-glucose units, provided by Roquette (France), with molecular mass $M_w = 2500$ g.mol^{-1}, dextrose equivalent DE $= 29$, and polydispersity index 4.9 (supplier data). The same batches were used throughout the experiments presented in this study and stored under vacuum with a dessicant to avoid any degradation. Maltodextrin is soluble in water and highly hygroscopic: the water content of the polymer equilibrates with the ambient humidity. The relative humidity of the atmosphere is defined as the ratio of the concentration of water in air to its concentration at saturation and equals the activity of water a_w, defined as the ratio between partial pressure of water in air and the saturated vapor pressure. At equilibrium, the activity of water in air and in the polymer are equal, and this sets the volume fraction of water in the polymer ϕ. The dependence of ϕ with a_w has been characterized experimentally (Dupas et al., 2013) and was found to be well described by a Flory equation: $a_w = \phi e^{1-\phi+\chi(1-\phi)^2}$, with a Flory parameter $\chi = 0.5$. Finally, the mutual diffusion coefficient D of water in maltodextrin has been measured by (Dupas et al., 2012). At room temperature, when the polymer is hydrated at a water volume fraction above 30%, the polymer is in a melt state. D varies between 2×10^{-11} m^2 s^{-1} for $\phi = 25\%$ and 10^{-10} m^2 s^{-1}, where it plateaus for water contents larger than $\phi = 50\%$. Therefore in all experiments performed at a humidity larger than 0.75 for which the water volume fraction is larger than 25%, we will consider D as a constant and $D = 10^{-10}$ m^2 s^{-1}. Supported films of the polymer were deposited on silicon substrates. Their thickness e was adjusted by using aqueous solutions of the polymer with concentration ranging between 1 and 40 wt% and with two different methods: spincoating of the aqueous solutions at 4000 rpm for thinner films and dipcoating for thicker ones. The thickness is measured by ellipsometry or interferometric profilometry and ranges from 100 nm to 8 μm. The layers are homogeneous across the central area of the wafer.

In specific cases we modify the surface properties of the solid underlying substrate by spincoating a 250-nm-thick layer of polystyrene (PS) in toluene on the silicon wafer. As it is, the PS layer is hydrophobic and the contact angle of water is $\theta_S = 90°$. By exposing the PS layer to a H_2O plasma for two different exposure times, we tune its hydrophobicity down to a contact angle of water of $\theta_S = 32°$ and $7°$, respectively. On these plasma-treated PS layers, maltodextrin solutions are spincoated as before. We thus obtain maltodextrin films on solid substrates of lesser hydrophilicity compared to the bare silicon wafers, as quantified by the values of θ_S. In all cases, the surface of these substrates is atomically smooth, and the good reflection of light at their surface allows for the precise measurement of the dynamic contact angle and of the film thickness at all times.

3.2 Procedures

Details on the experimental procedures have been published elsewhere (Dupas et al., 2013). The coated substrates are placed in a transparent sealed chamber (Fig. 2). A reservoir containing a saturated solution of chosen salt sets the humidity inside the box.[1] Humidity and temperature are monitored at all times with a sensor (Rotronics). Prior to any

[1]List of salts used and corresponding relative humidity RH: P_2O_5 (RH∼0), LiCl (RH=11%), K_2C0_3 (43%), NaBr (58%), NaCl (75%).

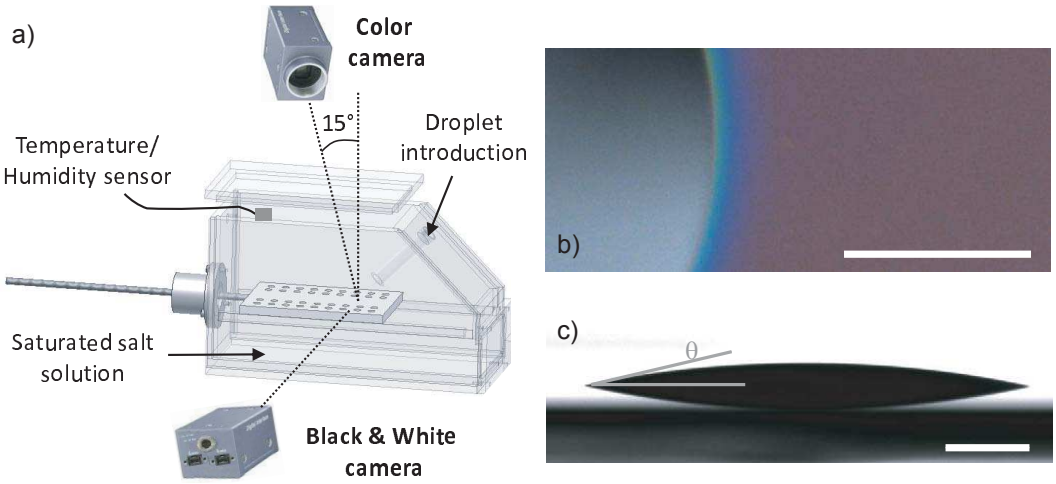

FIG. 2: (**a**) Experimental setup. (**b**) Top view of a spreading drop onto a 250-nm film of maltodextrin, $a_w = 0.43$. (**c**) Side view showing the determination of the dynamic contact angle θ. $e = 550$ nm, $a_w = 0.58$. Scale bars represent 1 mm.

experiment, the coated wafer is allowed to sit in the chamber until complete equilibration of the film with atmosphere. The experiment consists in depositing a 3-μL droplet on the coated substrate and monitoring its spreading from the side and the top with two synchronized cameras. The frame rate ranges between 1 and 30 Hz, depending on the spreading speed. Side illumination is provided by a white LED screen. The lateral views allow for an accurate determination of the dynamic contact angle θ of the droplet, as shown in Fig. 2(c). The top view [Fig. 2(b)] is acquired with a color camera placed at a 15° angle with respect to the vertical direction. The images show that the droplet shape remains circular during the whole spreading, with a radius R used to compute the contact line velocity $U = \dot{R}$. The spontaneous spreading of the sessile droplet yields contact line velocities ranging between 6×10^{-6} and 6×10^{-4} m/s. To explore faster contact line motion, we push the droplet with respect to the substrate by sliding the substrate backward at a controlled speed U while holding the liquid in place with a Teflon wiper tightly squeezed against the substrate. For this, a motor is attached to the platform slider and a high-speed camera (frame rate up to 150 Hz) monitors the side view. The contact line speeds relative to the substrate obtained this way range between approximately 5×10^{-4} and 0.7 m s^{-1}, but the contact line itself remains within the field of view of the camera. This experiment will be referred to as a pulled substrate experiment.

4. RESULTS

A typical result is shown in Fig. 3, where the contact angle θ is plotted as a function of the contact line speed U for a maltodextrin film of thickness $e \sim 250$ nm at different humidities. The film is initially equilibrated with the ambient humidity, and thus a higher a_w corresponds to a greater initial water content of the layer. Therefore, the contact angle is clearly sensitive to a change in the initial water content, and the wettability of the polymer is enhanced when hydration is greater. We now turn to the effect of the spreading velocity U. The spontaneous spreading of a water droplet starts fast and then, the spreading velocity decreases. In the meantime, we measure a decrease of the contact angle. We find that an increase in ambient humidity shifts the curves toward smaller θ values. Altogether, these measurements show that wettability is improved by hydration of the substrate, in agreement with our previous findings (Tay et al., 2010, 2011a; Dupas et al., 2013). Remarkably, as shown in the insert of Fig. 3 where higher velocities were obtained using the pulled substrate experiments, the contact angle reaches values as high as 110° for contact line velocities around 1 m/s, showing that very low hydrophilicity can be achieved at high speed. From high values of contact angle, we find that as the drop slows down, θ decreases and the wettability is enhanced.

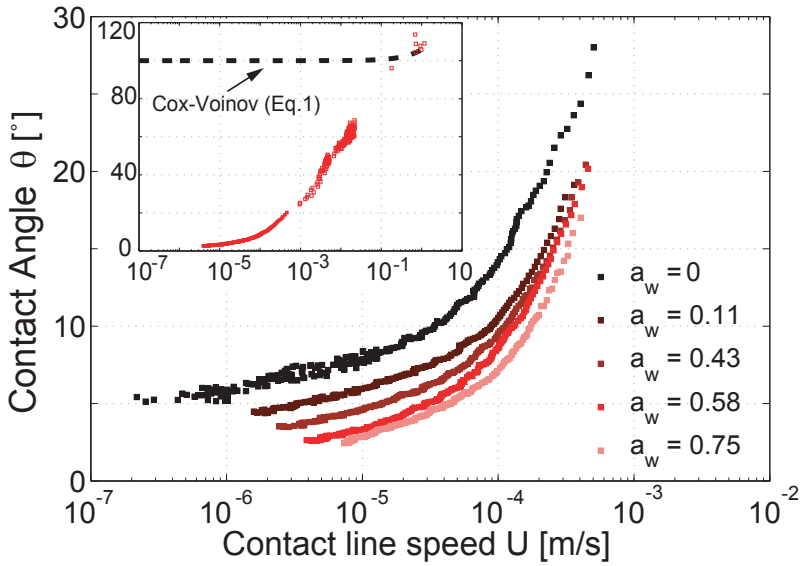

FIG. 3: Contact angle θ versus contact line speed U for droplets of water spreading on maltodextrin films of thickness $e = 250$ nm, at different water activities a_w for spontaneous spreading of sessile droplets. Higher humidity yields lower contact angles at a given U. (Insert) Data obtained with pulled substrates experiments (hollow symbols) are added to the spontaneous spreading data. At high speeds, within experimental accuracy, the contact angle keeps increasing with U and averages at $\theta = 110° \pm 5$ for $U \sim 0.7$ m s$^{-1} \pm 0.2$ for all humidities, a value even larger than 90°. Dashed line: Increase in contact angle θ as predicted by Eq. (1) accounting for the viscous effects only; $\eta = 10^{-3}$ Pa s. The curves clearly underestimate the observed change in θ.

Referring to Eq. (1), we can check that this effect is not due to the viscous dissipation term on the right-hand side of this equation. Indeed, we plot as a dashed line in Fig. 3 the variation of θ expected from the term $(\eta l U/\gamma)^{1/3}$ for a viscosity $\eta = 1$ mPa s and where $l = \ln(R/a) \sim 15$ in our experimental case. This term clearly underestimates the measured decrease of θ with decreasing U. Therefore, the variations of the contact angle can be attributed to the water transfers in the film that tune the term θ_e in Eq. (1), in agreement with previous findings (Dupas et al., 2013). These transfers depend on the relative values of the velocity at which the contact line moves and of the flux of water hydrating the film. For smaller velocities, the water flux hydrates the film in a longer time, and so the hydration is greater, yielding a smaller contact angle. A detailed analysis of the spreading dynamics of droplets on thin films (Dupas et al., 2013) showed that indeed, the contact angle θ is set by the water volume fraction in the polymer film at the contact line. This quantity depends on the initial water content absorbed by the polymer when in equilibrium with the atmosphere (thus, on the water activity a_w), and on the water transfers during the spreading of the droplet, that is, on e and U. It was even more demonstrated that, for thin enough films, θ is a function of the product eU, yielding $\theta = F(a_w, eU)$.

The top views of the spreading droplets clearly evidence the existence of water transfers into the polymer film in the vicinity of the contact line. Figure 2b shows a typical color image obtained during the spreading of a water droplet on a maltodextrin layer. Different hues can be seen in the film that are due to changes in thickness: the film is thin enough for interferences to build up between the two reflective interfaces, giving way to various hues that are directly related to the distance between the silicon surface and the upper polymer film surface. We check that the change in thickness can be attributed to a swelling of the polymer film by water rather than to a penetration of water between the film and the silicon substrate. In the latter case, the polymer would be peeled off the substrate and the moving contact line would actually connect the peeled polymer layer, the silicon wafer, and water. Therefore, the dynamic contact angle should be affected by a change in the silicon wafer surface energy. To check this hypothesis, we used the modified substrates for which a layer of polystyrene covers the silicon substrate. The dynamic contact

angles measured in the three cases are plotted as a function of the droplet velocity U in Fig. 4. We clearly find that the different substrates do not have any effect on the contact angle. We conclude here that the polymer layer is not peeled off the substrate and that water swells the polymer film in the vicinity of the droplet.

In another series of experiments, we varied the thickness of the film, keeping the humidity as a constant. The results are presented in Fig. 5(a) for maltodextrin films at humidity $a_w = 0.75$. Very similar results are obtained at other humidities. This series shows that the contact angles are shifted toward the larger values as the film thickness increases, in agreement with the results obtained earlier (Tay et al., 2010) describing how thicker films take longer to hydrate. However, the thickness no longer has an effect on these curves for the thicker films ($e = 2.7$ and 8 μm), for which, at velocities larger than 10^{-4} ms^{-1}, the θ-U curves superimpose. This defines the thick-film regime, for which the polymer film can be considered as a semi-infinite medium.

5. DISCUSSION

To compare our experimental data with the predictions by Tay et al. (2010), we have built e-U diagram in which we have reported the experimental iso-θ curves. First, the contact line speed U allows for the discrimination of a regime where the solvent uptake in the substrate is negligible, the "dry regime," and regimes where the solvent uptake is substantial. At contact line velocities larger than a critical velocity U_c the film remains essentially dry. For water and glassy maltodextrin, Tay et al. (2010) estimate U_c at 2×10^{-1} m s^{-1}. Here, the largest accessible velocity is 5×10^{-1} m s^{-1} (see Fig. 3 inset). Therefore, we are mostly interested in the "wet" regimes obtained below U_c.

As pointed out in what precedes, Tay et al. (2010) discriminated the thick regime from the thin regime by comparing the length x_c to a cutoff length ϵ of molecular size. A quick estimate and comparison with our experimental data show that this cutoff length is not the right choice to describe our results. Under this assumption, the transition between the thin and thick regime should happen for film thicknesses e such that $x_c = \epsilon$, that is $e > \sqrt{(\epsilon D)/U}$. With $\epsilon = 1$ nm, a diffusion coefficient of water in melt maltodextrin $D = 10^{-10}$m^2 s^{-1}, we would find a frontier between the two regimes at a film thickness $e_{\mathrm{thin/thick}} = 30$ nm for a typical velocity of 10^{-4} m s^{-1}. Given that the range of thicknesses tested in our experiments spans the 100 nm – 10 μm range, we should only probe the thick regime, for which no effect of the thickness is expected. This is clearly invalidated by the results of Fig. 5, where at

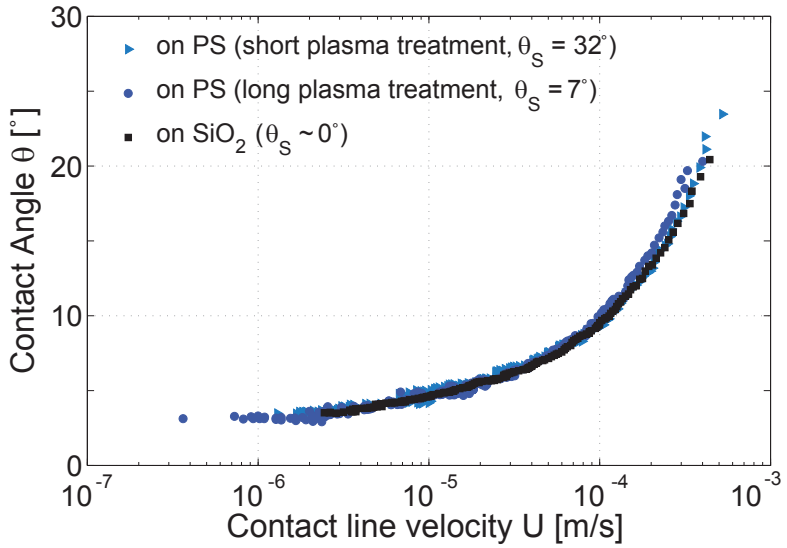

FIG. 4: Dynamic contact angle versus contact line speed during the spreading of a water droplet onto a film of maltodextrin DE29 deposited on substrates of various energy, as measured by the static contact angle of a water droplet on the substrates θ_S. No significant change in θ is observed from one substrate to another, demonstrating that the film is not peeled off the substrate.

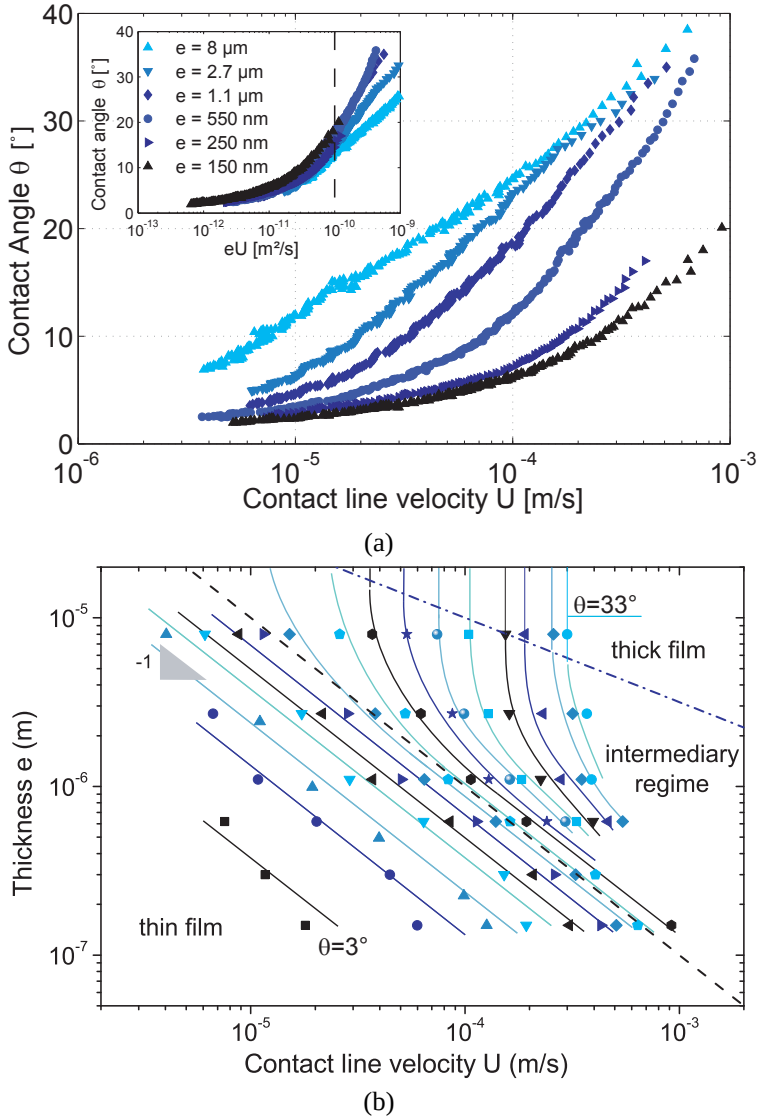

FIG. 5: $a_w = 0.75$ (**a**). Contact angle θ versus contact line speed U for droplets of water spreading on maltodextrin films of varied thickness e. Insert: Same data. Contact angle θ collapses on a single curve when plotted as the product of the thickness and the velocity eU as long as $eU < 10^{-10}$ m^2 s^{-1} (dashed line). This limit defines the frontier of the thin-film regime and compares to the prediction of Eq. (5) with good agreement. (**b**) Experimental iso-θ curves in a $e - U$ diagram for θ ranging between 3° and 33°, with steps of 2°. In the thin-film regime, the data are fit to a power law with exponent –1 (lines). Elsewhere, the lines serve as guides to the eyes. In the thick-film regime, vertical lines are expected since no dependence on e is expected. Dashed line: Frontier of the thin-film regime using $eU = 10^{-10}$ m^2 s^{-1} [see Fig. 5(a) inset and Eq. (5)]. Dashed-dotted line: Frontier of the thick-film regime according to Eq. (2) with $D = 10^{-10}$ m^{2}s^{-1}, $L = 10^{-4}$ m.

$U = 10^{-4}$ m s^{-1}, the θ-U curves only superimpose for thicknesses larger than $e = 2.7$ µm. This point emphasizes the need for a refined theory, which we present in the following. Our main findings are first that a cutoff length is provided by the length scale under which diffusion of water from the drop to the substrate is non-negligible, and second that

an intermediary regime between thin- and thick-film regimes has to be introduced. The two relevant length scales to which x_c must be compared to define those three regimes are κ, which is of the order the substrate thickness, and a macroscopic length L of the order of the droplet size.

5.1 Thick Regime

Let us first focus on the definition of the thick film regime. We consider the macroscopic length L, which is the distance at which the water content is set by the ambient atmosphere and not by the presence of the droplet (Sokuler et al., 2010). The distance L is the distance over which vapor diffuses in the air and can be easily measured on the color top images that show swelling of the polymer in the vicinity of the droplet (Dupas et al., 2013), an example of which is shown in Fig. 2(c). By comparing x_c to L, we find that if x_c is calculated to be larger than L, the bottom of the layer is never "seen" and the hydration adopts a diffusive profile along the vertical direction, as depicted in Fig. 6(a). In practice, the frontier defined by x_c cannot lay beyond L, by definition of L, and $x_c \sim L$. This situation is called the "thick regime," where e does not play a role. It is schematically depicted in Fig. 6(a). Experimentally, we find that at large velocities, and above a given thickness, the θ-U curves superimpose. This is typically the case for $e = 2.7$ μm and $e = 8$ μm for $a_w = 0.75$ and $U \sim 10^{-4}$ m/s. In the $e - U$ diagram, this leads to vertical iso-θ curves. For such values of e and U, we find that the contact angle is independent of the polymer thickness, and this defines the "thick-film regime." The limit of this regime can be found by comparing the distance to the contact line x_c, where the penetration of water by vertical diffusion is equal to the thickness e, to the macroscopic length L above

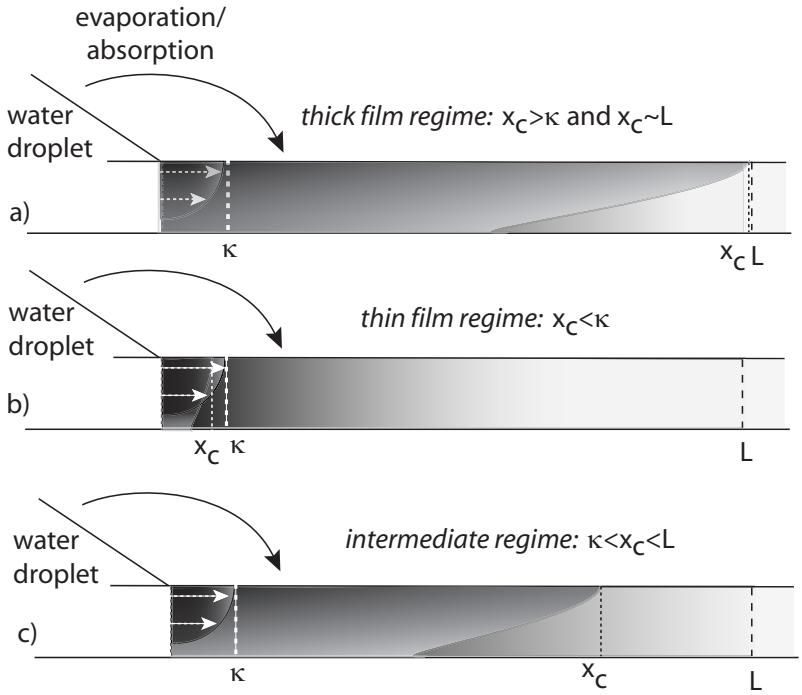

FIG. 6: Schematic representation of the water content in the layer ahead of the contact line, in the frame of reference of the droplet, where both evaporation/absorption and diffusion from the droplet are hydrating the film. L is the macroscopic length above which hydration is set by ambient humidity. ϵ is a nanometrer sized cutoff distance at which the water content sets the contact angle. κ is the extent of the penetration of liquid water by diffusion from the droplet, at the contact line. The diffusion of vapor from the atmosphere penetrates and homogenizes over a distance in the vertical direction that is larger than the film thickness for distances to the contact line larger than x_c. For smaller distances, the film exhibits a vertical gradient of water content.

which the substrate remains at equilibrium with the ambient atmosphere. In this way, the finite thickness of the film does not affect the water content of the polymer anywhere in the film. The thick-film regime is schematically depicted in Fig. 6(a). This leads to a criterion for the thick-film regime, $x_c \sim L$, yielding $e > e_{\mathrm{thick}}$, with

$$e_{\mathrm{thick}} = \sqrt{\frac{LD}{U}}. \tag{2}$$

In Fig. 5(b), we compare our experimental measurements to the prediction of Eq. (2) with $D = 10^{-10}$ m^2 s^{-1}, $L \sim 0.1$ mm. We find that the predicted frontier borders the experimental points for which the contact angle θ becomes independent of the thickness with a good agreement.

The water volume fraction in the thick-film regime can also be estimated. Indeed, a detailed calculation of the increase in water fraction $\Delta\phi$ for a thick film was derived (Tay et al., 2010) by integrating the flux of solvent arriving on the film by absorption of the evaporated water from the droplet at a distance from the contact line ranging between the macroscopic length L and the vicinity of the droplet (cutoff distance κ) [see Eq. (23) in that paper]. It yields, with $L \gg \kappa$,

$$\Delta\phi^{\mathrm{thick}} = K \frac{D_v c_{\mathrm{sat}}}{D^{1/2} \rho U^{1/2} \kappa^{1/2}}, \tag{3}$$

where $D_v = 2.6 \times 10^{-5}$ m^2 s^{-1} is the diffusion coefficient of vapor in the air, $c_{\mathrm{sat}} = 23.1$ g m^{-3} is the saturation concentration of water vapor in air, and $\rho = 10^3$ kg m^{-3} is the density of liquid water. The product $D_v c_{\mathrm{sat}}$ characterizes the transfer of evaporated water from the droplet by diffusion through the air. Note that the expression of $\Delta\phi$ involves a numerical factor K that depends on the sorption isotherm of water in the polymer. Therefore we are limited to scaling laws.

We now turn to the cases where the polymer thickness changes the spreading dynamics, namely, $e < e_{\mathrm{thick}}$. Among these, the thinnest polymer films can be homogeneously hydrated across their thickness, while the contact line of a water droplet advances. This is possible if the spreading dynamics is slow enough. A detailed analysis of this thin-film regime has been recently reported (Dupas et al., 2013) and allows for the definition of a quantitative criterion. Briefly, water transfers into the film through two mechanisms. First, water evaporates from the droplet, further condenses onto the polymer film, and diffuses vertically into the polymer. The water diffusion across the film is homogeneous as long as the distance to the contact line is larger than x_c. Second, liquid water diffuses into the polymer at the contact line of the droplet. Water diffuses from the droplet to a distance $\kappa = e[(D\rho)/(D_v c_{\mathrm{sat}})]$ smaller than e. Between 0 and κ, the water content of the polymer film originates in a balance between diffusion in air and in the polymer, and convection is negligible. As a result, in the vicinity of the contact line, the water transferred in the polymer film is independent of e and of U. This situation is depicted in Fig. 6, where the liquid water diffuses into the polymer at the contact line over the distance κ.

5.2 Thin Regime

By comparing the two relevant distances x_c and κ, we are able to define a criterion for when the spreading dynamics occurs in the thin-film regime: when $x_c < \kappa$ [see Fig. 6(b)], at any distance to the contact line, the water fraction in the polymer film is inversely proportionate to the polymer volume, that is, to e. It was shown (Tay et al., 2010, 2011a; Dupas et al., 2013) that the dynamic contact angle varies as $1/(eU)$ in this case. The inset of Fig. 6 presents the experimental measurements of θ plotted against the product eU. All the data collapse on a master curve for small enough values of eU. The criterion for the thin-film regime, $x_c < \kappa$, yields $e < e_{\mathrm{thin}}$, with

$$e_{\mathrm{thin}} = D/U \frac{D\rho}{D_v c_{\mathrm{sat}}}, \tag{4}$$

$$(eU)_{\mathrm{thin}} = D \frac{D\rho}{D_v c_{\mathrm{sat}}}. \tag{5}$$

This prediction was compared to our experimental data. From the insert in Fig. 5, we find that the contact angle no longer follows a master curve in eU when $eU \sim 10^{-10}$ m^2 s^{-1}. From Eq. (5), with a mutual diffusion coefficient of

water in melt maltodextrin taken as $D = 10^{-10}$ m^2 s^{-1}, our model predicts $(eU)_{\rm thin} = 2 \times 10^{-11}$ m^2 s^{-1}. There is therefore a reasonable agreement of the prediction with the experimental results. The discrepancy between the model and the measurements can be reconciled by changing the cutoff distance for the regime change from κ to a few times κ (namely, $\sim 5\kappa$ from data), which is reasonable in analyses using scaling laws as in here.

The increase of water volume fraction in the thin-film regime can also be estimated. Using again the calculation derived by Tay et al. (2010), the flux of solvent arriving on the film by absorption of the evaporated water from the droplet is integrated over distances from the contact line ranging between the macroscopic distance L and the cutoff distance κ, with the difference that for thin films, the whole thickness of the film is hydrated and the vertical penetration depth for water is exactly the thickness e. Using Eq. (21) in the work of Tay et al. (2010), we modify the expression to account for the new microscopic cutoff length, taken as κ. The result is

$$\Delta\phi^{\rm thin} \sim \frac{D_v c_{\rm sat}}{\rho U} \frac{1}{e} \ln\left(\frac{e_{\rm thick}}{e_{\rm thin}}\right), \tag{6}$$

where $D_v = 2.6 \times 10^{-5}$ m^2 s^{-1}, $c_{\rm sat} = 23.1$ g m^{-3}, and $\rho = 10^3$ kg m^{-3}, and $\ln(e_{\rm thick}/e_{\rm thin}) = 1/2 \ln(L/\kappa)$ is typically of order 1 in our conditions. The scaling in $1/eU$ mentioned above is explicit in this equation.

5.3 Intermediary Regime

From the present analysis, an intermediary regime arises that has never been described. It corresponds to spreading experiments where the polymer film presents two different zones for hydration: close to the contact line, the film exhibits a vertical gradient of water volume fraction, while at larger distances, diffusion across the film thickness gives way to a uniform water content along the film depth. This regime is obtained for thicknesses e such that $e_{\rm thin} < e < e_{\rm thick}$. In the series of data collected for varied polymer film thicknesses, it corresponds to cases where the $\theta - U$ curves do not superimpose and the θ versus eU curves do not collapse either, visible in Fig. 5. The intermediate regime is schematically depicted in Fig. 6(c).

The water fraction in the intermediary regime can also be derived based on the equations of the paper by Tay et al. (2010). It involves two distinct terms, the first describing the part of the layer that is fully hydrated and the second, the partially hydrated layer, yielding a combination of Eqs. (6) and (3). We find

$$\Delta\phi^{int} = K \frac{D_v c_{\rm sat}}{\rho U} \frac{1}{e} \left[ln\left(\frac{e_{\rm thick}}{e}\right) + \frac{e}{e_{\rm thin}} - 1 \right]. \tag{7}$$

6. CONCLUSIONS

In this study, we provide a comprehensive description of the transfers relevant to the problem of the spreading of a droplet onto a soluble polymer film. We demonstrate that the variations of the dynamic contact angle are set by the water content of the substrate. We show that three different transfers are at stake between the droplet and the soluble substrate: (i) water evaporates from the droplet, condenses on the substrate, and further diffuses into the polymer; (ii) water is convected at a velocity U, the contact line speed; and (iii) liquid water diffuses into the polymer from the liquid wedge at the contact line. Although the evaporation flux provides a quantity of water that diverges at the contact line (Dupas et al., 2013), we show how the diffusive process of liquid water at the contact line introduces a cutoff length κ. The length κ compares the fluxes of water arriving by diffusion through the air and through the polymer. Beyond κ, water molecules in the substrate are at equilibrium with the atmosphere and convection is negligible. Therefore, this characteristic length is the distance to the contact line where the volume fraction of water sets the substrate energy experienced by the droplet and thus the dynamic contact angle. As a consequence, by comparing the penetration depth x_c to the macroscopic cutoff length L set by the extent of the evaporative flux, and to the microscale cutoff length κ, we were able to map out three different regimes of spreading of a droplet on a soluble substrate. The regimes depend on the values of the substrate thickness e and the contact line velocity U that characterize the transfers by convection and by evaporation.

At small e and U, a thin-film regime is obtained. It is characterized by a homogeneous hydration of the film across its thickness, and the dynamic contact angle is a function of the product eU. For large thicknesses and large velocities, hydration of the substrate is weak and barely penetrates into the film along the vertical direction. The solid behaves as a semi-infinite medium with a dynamic contact angle that does not depend on the thickness e: this is the thick-film regime. The flux of water through the vapor phase hydrates the substrate at all distances to the contact line ranging between a molecular cutoff and the macroscopic cutoff L, and the resulting water volume fraction in the polymer is set by a balance of the condensation flux and the convection at velocity U. Therefore, in the thick-film regime, the contact angle and the water volume fraction depend on the velocity U only. Between the thin and thick regimes, an intermediate case arises where two distinct areas coexist in the film away from the contact line: close to the droplet, the film exhibits a gradient of water concentration along the thickness, and at larger distances, a homogeneous water content along the vertical direction is obtained. The frontier between the thin and intermediary regimes was successfully predicted by comparing x_c to the microscale cutoff length κ while the frontier between the intermediary and thick film regimes was obtained by comparing x_c to the macroscopic cutoff distance L.

Altogether, the spreading dynamics of a solvent droplet on a soluble polymer of low molecular mass is now well understood. Extensions of this study include the effect of viscoelastic effects at the contact line that could arise from the use of polymer of larger masses that develop a gelphase with low dissolution kinetics. The onset of such a gel phase is expected to introduce a new cutoff length in the problem. Another aspect yet to be studied is the transition from a glassy to a melt state for initially dry polymers. Indeed, it is commonly observed that hydrosoluble polymers of glass transition temperature T_g close to ambient temperature undergo a glass transition in water content: the T_g decreases as their water content increases. These aspects are to be developed in coming studies.

REFERENCES

Carre, A. and Shanahan, M., Direct evidence for viscosityindependent spreading on a soft solid, *Langmuir*, vol. **11**, no. 1, pp. 24–26, 1995.

Chen, L., Bonaccurso, E., and Shanahan, M. E. R., Inertial to viscoelastic transition in early drop spreading on soft surfaces, *Langmuir*, vol. **29**, no. 6, pp. 1893–1898, 2013.

de Gennes, P. G., Wetting: Statics and dynamics, *Rev. Mod. Phys.*, vol. **57**, no. 3, pp. 827–863, 1985.

Dupas, J., Wetting of Soluble Polymers, PhD Thesis, Universite Pierre et Marie Curie (UPMC), Paris, France, 2012.

Dupas, J., Verneuil, E., Ramaioli, M., Forny, L., Talini, L., and Lequeux, F., Dynamic wetting on thin film of soluble polymer: Effects of non-linearities in the sorption isotherm, *Langmuir*, vol. **29**, pp. 12572–12578, 2013.

Kajiya, T., Daerr, A., Narita, T., Royon, L., Lequeux, F., and Limat, L., Dynamics of the contact line in wetting and diffusing processes of water droplets on hydrogel pamps paam substrates, *Soft Matter*, vol. **7**, no. 24, pp. 11425–11432, 2011.

Kajiya, T., Daerr, A., Narita, T., Royon, L., Lequeux, F., and Limat, L., Advancing liquid contact line on visco-elastic gel substrates: Stick-slip vs. continuous motions, *Soft Matter*, vol. **9**, no. 2, pp. 454–461, 2013.

Leger, L. and Joanny, J., Liquid spreading, *Reports Prog. Phys.*, vol. **55**, no. 4, pp. 431–486, 1992.

Long, D., Ajdari, A., and Leibler, L., Static and dynamic wetting properties of thin rubber films, *Langmuir*, vol. **12**, no. 21, pp. 5221–5230, 1996.

Monteux, C., Tay, A., Narita, T., De Wilde, Y., and Lequeux, F., The role of hydration in the wetting of a soluble polymer, *Soft Matter*, vol. **5**, no. 19, p. 3713, 2009.

Muralidhar, P., Bonaccurso, E., Auernhammer, G. K., and Butt, H.-J., Fast dynamic wetting of polymer surfaces by miscible and immiscible liquids, *Colloid Polym. Sci.*, vol. **289**, pp. 1609–1615, 2011.

Sokuler, M., Auernhammer, G. K., Liu, C. J., Bonaccurso, E., and Butt, H.-J., Dynamics of condensation and evaporation: Effect of inter-drop spacing, *EPL*, vol. **89**, no. 3, 2010.

Tay, A., Monteux, C., Bendejacq, D., and Lequeux, F., How a coating is hydrated ahead of the advancing contact line of a volatile solvent droplet, *EPJ E*, vol. **33**, no. 3, p. 8, 2010.

Tay, A., Bendejacq, D., Monteux, C., and Lequeux, F., How does water wet a hydrosoluble substrate? *Soft Matter*, vol. **7**, no. 15, p. 6953, 2011a.

Tay, A., Lequeux, F., Bendejacq, D., and Monteux, C., Wetting properties of charged and uncharged polymeric coatings–effect of the osmotic pressure at the contact line, *Soft Matter*, vol. **7**, no. 10, pp. 4715–4722, 2011b.

Zuo, B., Qian, C., Yan, D., Liu, Y., Liu, W., Fan, H., Tian, H., and Wang, X., Probing glass transitions in thin and ultrathin polystyrene films by stick-slip behavior during dynamic wetting of liquid droplets on their surfaces, *Macromolecules*, vol. **46**, no. 5, pp. 1875–1882, 2013.